Hybrid Aminoquinoline-Triazine Ligand Design: Synthesis, Characterisation, and Coordination Chemistry with Platinum-Group Metal Precursors

Paige S. Zinman,[1] Gregory S. Smith[1,*]

[1]*Department of Chemistry, University of Cape Town, Rondebosch, South Africa*

ABSTRACT

The synthesis and characterisation of a trimeric aminoquinoline-triazine hybrid ligand and the corresponding half-sandwich trimetallic platinum-group metal complexes are described. The incorporation of the 1,3,5-triazine structure allowed for the formation of a symmetrical trimeric ligand, from which corresponding iridium(III), rhodium(III) and ruthenium(II) trinuclear complexes were synthesised. The synthesis of the ligand was achieved *via* a nucleophilic aromatic substitution reaction of the 4-aminoquinoline precursor with 2,4,6-trichloro-1,3,5-triazine. The complexation reactions of the monodentate trimeric ligand with the appropriate precursor dimers $[IrCp^*(\mu\text{-}Cl)Cl]_2$ (Cp^* = pentamethylcyclopentadienyl), $[RhCp^*(\mu\text{-}Cl)Cl]_2$ and $[Ru(p\text{-cymene})(\mu\text{-}Cl)Cl]_2$ afforded three new half-sandwich trimetallic complexes. The complexes are moisture and air-stable, however are insoluble in most organic and aqueous solvents except for highly polar solvents such as DMSO. To corroborate and clarify the proposed structures of the synthesised compounds, an array of spectroscopic and analytical techniques, including solid-state NMR experiments, were utilised.

KEYWORDS

Polymetallic, Microwave synthesis, Spectroscopy, Solid-state NMR

Received 17 February 2025, revised 13 October 2025, accepted 30 October 2025

INTRODUCTION

The diverse applications of transition metals to fields such as catalysis and biology demonstrates the benefit and need for the facile development of effective organometallic complexes. Transition metal complexes are greatly versatile with the tuning of structural or chemical properties achieved by simple ligand modifications and their abilities for metal-ion exchange.[1,2] The diverse geometries, stereochemistry and molecular complexities generated by metal-based complexes are not usually possible for purely organic molecules.[3, 4] Additionally, the electronic properties of d-block metal complexes can be tailored for ideal chemical reactivities and physical properties.[5, 6] Moreover, metal complexes have been documented to exhibit improved reversible redox behaviour and increased stability compared to organic systems.[7]

The development of multinuclear complexes has flourished due to their enhanced reactivities relative to their mononuclear counterparts across many industries.[8] Polynuclear complexes are structurally bulkier, they bear multiple active sites and exhibit improved stability compared to mononuclear complexes.[9-11] Furthermore, polynuclear complexes have exceptional redox and optical properties favourable for photo-induced catalytic applications.[11-14]

The triazine molecule is a planar, six-membered, benzene-like ring which is composed of three nitrogen and three carbon atoms.[15] These heterocycles are strongly electron-withdrawing owing to the three contained nitrogen atoms and substitution of a leaving group attached to the triazine ring generally occurs easily without the aid of a catalyst.[16] There are three regioisomers of triazine namely; 1,2,3-triazine, 1,2,4-triaine and 1,3,5-triazine.[17] The three-fold symmetrical nature of the 1,3,5-triazine isomer, otherwise known as *s*-triazine, makes it a useful and versatile scaffold for synthetic chemistry, due to the lack of regiochemical concerns as well as its increased stability.[18] 2,4,6-Trichloro-1,3,5-triazine, commonly known as cyanuric chloride, is a derivative of 1,3,5-triazine and is often utilised for organic synthetic applications which are selective, mild in conditions, inexpensive and non-toxic.[19] The chlorine atoms attached to the triazine core of cyanuric chloride have different reactivities which is useful for the sequential introduction of various substituents in combinatorial synthesis. However, the displacement of the third chlorine atom often presents as a challenge without the exploitation of microwave heating to assist in improving the reaction yields and kinetics of these notoriously sluggish reactions.[20-22] While *s*-triazine is a versatile entity within synthetic chemistry, it also holds great potential for material chemistry owing to their coordination, hydrogen bonding and π-interaction capabilities.[23,24] The synthesis of a number of organic di- and tri-substituted triazines that lack transition metal incorporation have been previously reported.[25-31] Additionally, polynuclear triazine-based complexes have been frequently studied within the supramolecular chemistry fields.[32,33]

Multiple detailed studies have investigated the internal rotation of substituents attached to triazine ring systems. As a result, rotational isomers are formed and cause rotamer exchange effects on the solution-state NMR spectra.[34-36] Consequently, IR and solid-state NMR studies are among the most popular techniques used for the characterisation of tri-substituted triazine compounds.[34,37,38] The versatility of triazines is exemplified by their array of chemical applications within the agricultural, electrochemical, crystal engineering and biochemical fields.[18,19,39] Moreover, the triazine scaffold is contained in numerous biologically active molecules which possess anti-convulsive,[16] anti-inflammatory,[40,41] anti-tubercular,[42] anti-bacterial,[43,44] anti-viral[45,46] and anticancer[44,47] properties.

Quinoline is a well-established and versatile scaffold in medicinal chemistry, forming a key part of a notable group of heterocyclic compounds with impressive pharmacological activity.[48,49] The aminoquinoline motif is notably present in the well-known antimalarial drug chloroquine.[50] The research groups of Manohar *et al.* and Melato *et al.* have reported on the synthesis of hybrid organic triazine-based compounds that incorporate aminoquinoline groups.[21,51-54] This study focused on synthesising and characterising a trimeric aminoquinoline-triazine hybrid ligand, along with its corresponding tri-homonuclear complexes of iridium(III), rhodium(III), and ruthenium(II).

EXPERIMENTAL

General methods and chemicals

All reagents and solvents were commercially sourced (Sigma-Aldrich, Merck and Kimix) and used without further purification.

*To whom correspondence should be addressed
Email: gregory.smith@uct.ac.za

ISSN 1996-840X Online / South African Chemical Institute / http://saci.co.za/journal

https://doi.org/10.17159/0379-4350/2025/v79a16

Iridium(III) trichloride trihydrate, rhodium(III) trichloride trihydrate and ruthenium(II) trichloride trihydrate were purchased from Heraeus SA. The $[Ru(p\text{-cymene})(\mu\text{-Cl})Cl]_2$, $[IrCp^*(\mu\text{-Cl})Cl]_2$ (**3**), and $[RhCp^*(\mu\text{-Cl})Cl]_2$ dimeric precursors, and the ligand precursor *N*^{1}-(7-chloroquinolin-4-yl)propane-1,3-diamine (**1**) were prepared following literature methods.[55-57] All solvents used were reagent grade. The solvents specifically used in the purification and extraction steps were dried over molecular sieves. All aqueous solutions (NaOH, NaCl, $NaHCO_3$) were prepared using deionised water. Synthetic procedures were carried out under nitrogen atmosphere using standard Schlenk line techniques unless otherwise stated. Reactions were monitored by thin-layer chromatography (TLC) using aluminium-backed precoated silica gel 60 F254 or neutral alumina oxide 60 F254 plates and viewed under ultraviolet (UV) light at 254 nm. Microwave-assisted reactions were carried out in a single-mode CEM Discover SP Microwave Synthesizer. Incident power and temperature were controlled by computer using the CEM Synergy™ software.

Spectroscopic and analytical techniques

Nuclear magnetic resonance (NMR) spectra were obtained on a Bruker XR600 MHz spectrometer (^{1}H at 599.95 MHz and $^{13}C\{^1H\}$ at 151.0 MHz), a Bruker XR400 spectrometer (^{1}H at 399.95 MHz and $^{13}C\{^1H\}$ at 100.58 MHz) or a Varian Mercury 300 (^{1}H at 300.08 MHz) spectrometer. Chemical shifts are recorded in ppm (δ) and *J*-coupling values reported in Hz with tetramethylsilane (TMS) used as the internal standard. The signals are designated as follows: s, singlet; d, doublet; dd, doublet of doublets; dt, doublet of triplets; t, triplet; m, multiplet; br.s, broad singlet.

Solid-state NMR experiments were recorded at 298K on a 500 MHz Bruker AVANCE III HD operating at 11.7 T. Using 2.5 mm diameter zirconia rotors (Bruker, Karlsruhe, Germany), the spectra were obtained at a spinning rate of 20 kHz on a broad band triple resonance Trigamma probe operating in the ^{1}H/^{13}C/^{15}N mode. The data was acquired using a standard cross polarisation magic-angle spinning solid-state ^{13}C spectra (^{13}C CP(MAS)) sequence using a 4.0 µs proton 90° pulse, 2.0 ms contact pulse, a broadband decoupling sequence (SPINAL64) and a repetition delay of 3 s to accumulate 18000 scans. ^{1}H spectra were acquired using a standard one-pulse sequence. Glycine was used to achieve the Hartman-Hahn matching conditions and as an external standard for the calibration of the chemical shift.

Infrared (IR) spectroscopy was conducted using a Perkin-Elmer Spectrum 100 FT-IR spectrometer fitted with an Attenuated Total Reflectance (ATR) unit and with bond vibrations measured in reciprocal centimetres (cm^{-1}). Melting points were measured using a Büchi Melting Point Apparatus B-540 and are uncorrected. Purity was determined using an analytical Agilent HPLC 1260 equipped with an Agilent infinity diode array detector (DAD) 1260 UV-Vis detector, with an absorption wavelength range of 210-640 nm. The compounds were eluted using a mixture of solvent A (10 mM NH_4OAc/H_2O) and solvent B (10 mM NH_4OAc/MeOH) at a flow rate of 0.9 mL min^{-1}. The gradient elution conditions were as follows: 10% solvent B from 0 – 1 min, 10 – 95% solvent B from 1 – 3 min, 95% solvent B from 3 – 5 min. High resolution (HR) electrospray ionisation mass spectrometry (ESI-MS) was performed on a Waters Synapt G2 mass spectrometer equipped with an ESI probe and with data recorded using the positive mode.

Synthesis of N²,N⁴,N⁶-tris(3-((7-chloroquinolin-4-yl)amino) propyl)-1,3,5-triazine-2,4,6-triamine (2)

In a 10 mL microwave capped vial NaOH (1 equiv.) was added to a solution of cyanuric chloride (0.238 g, 1.29 mmol) in 3.00 mL dry DMF, followed by the addition of 3 equiv. of precursor **1** (0.915 g, 3.88 mmol) whilst stirring at ambient temperature. The vial was microwave-irradiated at 150 °C (measured by the internal infrared sensor) at 6 bar pressure for 20 min within the microwave cavity. The reaction mixture was cooled to room temperature followed by precipitation by the drop-wise addition of saturated aqueous $NaHCO_3$ solution (10.0 mL). The product was isolated by vacuum filtration and washed with cold water and dried *in vacuo*. Compound **2** was isolated as a light green solid. Yield: 0.397 g (39%). ^{1}H NMR (300 MHz, DMSO-d_6): δ (ppm) = 8.39 (3H, d, *J* = 5.4 Hz, H_b), 8.25 (3H, d, *J* = 9.0 Hz, H_g), 8.14 (3H, s, H_n), 7.78 (3H, d, *J* = 1.9 Hz, H_d), 7.45 (3H, dd, *J* = 9.0, 1.9 Hz, H_f), 7.33 (3H, t, *J* = 5.2 Hz, H_j), 6.47 (3H, d, *J* = 5.4 Hz, H_a), 3.29 (6H, m, H_k), 3.21 (6H, m, H_m), 1.80 (6H, p, *J* = 6.9 Hz, H_l). $^{13}C\{^1H\}$ NMR (101 MHz, DMSO-d_6): δ (ppm) = 161.29 (C-o), 151.98 (C-b), 150.08 (C-i), 149.11 (C-c), 133.24 (C-e), 127.53 (C-d), 124.13 (C-f), 124.10 (C-g), 117.52 (C-h), 98.70 (C-a), 38.90 (C-k), 35.14 (C-m), 27.79 (C-l). ^{13}C NMR (CP-MAS, 500 MHz): δ (ppm) = 162.69 (C-o), 149.19 (C-b), 147.46 (C-e,i), 133.39 (C-c,d), 124.69 (C-f,g), 115.94 (C-h), 96.82 (C-a), 40.56 (C-k), 36.97 (C-m), 27.57 (C-l). IR (ATR): (ν_{max}/cm^{-1}) 3300 (*sec.* N-H), 1654 $(C{=}N)_{triazine}$, 1561 $(C{=}N)_{quinoline}$. Melting point: 245.3-246.5 °C. MS (ESI, *m/z*): 271.2 (35%, $[M + Cl - 2H]^{3-}$), calculated 271.9; 390.0 (5%, $[M - 2H]^{2-}$), calculated 390.1. MS (HR-ESI, *m/z*): 446.9036 (75%, $[M + MeCN + 2Cl]^{2-}$), calculated 447.0630; 604.8542 (20%, $[M - C_9H_6N_2Cl]^-$), calculated 604.5940; 780.8481 (15%, $[M - H]^-$), calculated 781.2030.

Synthesis of trinuclear aminoquinoline-triazine hybrid complexes (3-5)

Ir(III) aminoquinoline-triazine complex (3)

A solution of ligand **2** (0.112 g, 0.143 mmol) and metal precursor $[IrCp^*(\mu\text{-Cl})Cl]_2$ (**3**) (0.171 g, 0.214 mmol) was prepared in anhydrous acetonitrile (20.0 mL). The reaction mixture was stirred at room temperature for 16 h. A bright yellow precipitate formed, which was then filtered and washed with acetonitrile. The Ir(III) complex (**3**) was isolated as a solvate, $3\bullet(CH_3CN)_x$, with x indicating the stoichiometric ratio of acetonitrile to the complex, as observed from the NMR data. Complex **3** was obtained as a bright yellow solid. Yield: 0.234 g (77%). ^{1}H NMR (300 MHz, DMSO-d_6): δ (ppm) = 8.41 (3H, d, *J* = 5.6 Hz, H_b), 8.29 (3H, d, *J* = 9.0 Hz, H_g), 8.14 (3H, s, H_n), 7.79 (3H, s, H_d), 7.55 (3H, t, *J* = 4.3 Hz, H_j), 7.49 (3H, dd, *J* = 9.0, 2.0 Hz, H_f), 6.52 (3H, d, *J* = 5.6 Hz, H_a), 3.36-3.26 (6H, m, H_k), 3.21 (6H, q, *J* = 6.6 Hz, H_m), 1.87-1.74 (6H, m, H_l), 1.62 (45H, s, H_q). ^{13}C NMR (CP-MAS, 500 MHz) δ (ppm) = 161.80 (C_o), 157.78 (C_b), 150.43 (C_i), 147.04 (C_e), 133.77 (C_c), 128.24 (C_d), 123.42 (C_f), 121.49 (C_g), 116.02 (C_h), 99.91 (C_a), 86.08 (C_p), 41.55 (C_k), 37.58 (C_m), 28.08 (C_l), 9.48 (C_q). IR (ATR): (ν_{max}/cm^{-1}) 3324 (*sec.* NH), 1676 $(C{=}N)_{triazine}$, 1564 $(C{=}N)_{quinoline.}$ Melting point: 249.9-250.6 °C. MS (HR-ESI, *m/z*): 626.1290 (30%, $[M + CH_3CN + 3Na^+]^{3+}$), calculated 625.6087.

Rh(III) aminoquinoline-triazine complex (4)

Ligand **2** (0.0880 g, 0.113 mmol) was dissolved in dry methanol (10.0 mL). To this solution, $[RhCp^*(\mu\text{-Cl})Cl]_2$ (0.105 g, 0.170 mmol) was added, and the mixture was stirred for 16 h at room temperature. Once completed, the reaction vessel was placed in an ice bath, promoting formation of a precipitate which was filtered under vacuum and washed with cold methanol. The resulting solid was dried under reduced pressure. Complex **4** was obtained as an orange powder. Yield: 0.0923 g (47%). ^{1}H NMR (300 MHz, DMSO-d_6): δ (ppm) = 8.39 (3H, d, *J* = 5.1 Hz, H_b), 8.25 (3H, d, *J* = 9.0 Hz, H_g), 8.12 (3H, s, H_n), 7.78 (3H, s, H_d), 7.46 (3H, d, *J* = 8.7 Hz, H_f), 7.33 (3H, s, H_j), 6.48 (3H, d, *J* = 5.3 Hz, H_a), 3.27 (6H, m, H_k), 3.20 (6H, m, H_m), 1.80 (6H, m, H_l), 1.62 (45H, s, H_q). ^{13}C NMR (CP-MAS, 500 MHz) δ (ppm) = 161.64 (C_o), 158.18 (C_b), 150.66 (C_i), 147.01 (C_e), 133.44 (C_c), 127.39 (C_d), 124.02 (C_f), 121.33 (C_g), 116.57 (C_h), 100.22 (C_a), 94.46 (C_p), 41.74 (C_k), 37.59 (C_m), 28.41 (C_l), 9.68 (C_q). IR (ATR): (ν_{max}/cm^{-1}) 3312 (*sec.* NH), 1654 $(C{=}N)_{triazine}$, 1578 $(C{=}N)_{quinoline}$.

Melting point: > 266.5 °C dec. without melting. MS (HR-ESI, *m/z*): 536.0757 (50%, $[M + CH_3CN + 3Na^+]^{3+}$), calculated 536.2987.

Ru(II) aminoquinoline-triazine complex (5)

Ligand **2** (0.0955 g, 0.122 mmol) was dissolved in acetonitrile (30.0 mL). To this solution, a slight excess of $[Ru(p\text{-cymene})(\mu\text{-Cl})Cl]_2$ (0.119 g, 0.194 mmol) was added, and the mixture was allowed to stir for 16 h at room temperature. The solvent was removed by rotary evaporation, the remaining solid was re-dissolved in dichloromethane (DCM) and brown insoluble residues were removed by filtration. Thereafter, the filtrate was concentrated under reduced pressure and layered with diethyl ether. The resulting precipitates were collected by vacuum filtration and washed with diethyl ether (5.00 mL). Complex **5** was obtained as a dark orange powder. Yield: 0.0507 g (24%). ^{1}H NMR (300 MHz, CD_3OD): δ (ppm) = 8.39 (6H, m, $H_{b,g}$), 7.86 (3H, s, H_d), 7.68 (3H, d, *J* = 8.9 Hz, H_f), 6.85 (3H, d, *J* = 6.9 Hz, H_a), 5.71 (2H, d, *J* = 5.9 Hz, H_s), 5.57 (2H, d, *J* = 5.8 Hz, H_s), 5.49 (2H, d, *J* = 6.0 Hz, H_s), 5.43 (2H, d, *J* = 5.9 Hz, H_s), 5.29 (2H, d, *J* = 6.0 Hz, H_s), 5.23 (2H, d, *J* = 5.8 Hz, H_s), 3.61 (6H, t, *J* = 6.9 Hz, H_k), 3.39 (6H, t, *J* = 6.7 Hz, H_m), 2.78 (3H, m, H_q), 2.20 (6H, s, H_u), 2.19 (3H, s, H_u), 2.06-1.93 (6H, m, H_l), 1.26 (18H, m, H_p). ^{13}C{^{1}H} NMR (151 MHz, CD_3OD): δ (ppm) = 164.34, 157.56, 144.13, 140.92, 140.38, 128.69, 125.90, 120.56, 117.08, 99.72, 98.51, 94.75, 79.76, 78.59, 78.55, 77.65, 77.44, 42.21, 36.34, 32.74, 28.99, 27.56, 22.45, 18.79. IR (ATR): (ν_{max}/cm^{-1}) 3274 (*sec.* NH), 1666 $(C=N)_{triazine}$, 1588 $(C=N)_{quinoline}$. Melting point: > 193 °C dec. with onset of melting. MS (HR-ESI, *m/z*): 590.9619 (50%, $[M + MeOH + 3Na^+]^{3+}$), calculated 591.1687.

RESULTS AND DISCUSSION

The synthesis of the trimeric 4-amino-7-chloroquinoline-1,3,5-triazine ligand (**2**) required two synthetic steps, as outlined in Scheme 1. The first step involved the synthesis of *N*^{1}-(7-chloroquinolin-4-yl)propane-1,3-diamine (**1**) *via* a nucleophilic aromatic substitution (S_NAr), from 4,7-dichloroquinoline and excess 1,3-diaminopropane following a method published in the literature.[57] The obtained spectroscopic and analytical data for the 4-amino-7-chloroquinoline derivative (**1**) is comparable to that reported in the literature (Figure 1).[57,58]

The second step involved utilizing microwave irradiation for the reaction of precursor **1** with cyanuric chloride *via* a S_NAr reaction following the methodology of Melato *et al.* [21] which produced a homo-trisubstituted triazine derivative (**2**). The microwave-assisted reaction proceeded quickly, resulting in a pale-green solid in moderate yield of 39%.

The synthesis of the trinuclear iridium(III), rhodium(III) and ruthenium(II) 4-amino-7-chloroquinoline-triazine complexes (**3-5**) were all achieved *via* a simple entropically driven bridge-splitting metal complexation reaction (Scheme 1). The synthesis of the three varying metal complexes followed mild conditions which have been published in literature.[59,60] The Ir(III), Rh(III) and Ru(II) trinuclear metal complexes were isolated as bright yellow, orange and pale-orange powders, respectively, in low to good yields of 22-91%.

Analysis of the ^{1}H NMR spectrum (Figure 1) of the 7-chloroquinoline precursor (**1**) revealed five aromatic signals resonating between 8.38 ppm and 6.46 ppm, which were assigned to the protons of the quinoline core. Additionally, three aliphatic signals resonating at 1.73 ppm, 2.69 ppm and 3.32 ppm, were assigned to the protons of the propyl chain appended to the secondary amine on the 4-position of the quinoline scaffold.

Upon comparison of the ^{1}H NMR spectrum of precursor **1** (Figure 1a) to that of the corresponding trimeric 7-chloroquinoline-1,3,5-triazine ligand (**2**) (Figure 1b) a significant downfield shift is observed of the aliphatic signal assigned to the propylene proton (H_m) closest to the secondary nitrogen adjoining the triazine motif to the quinoline core, from 2.69 ppm to 3.21 ppm. Notably, the spectrum of ligand **2** shows a new resonance at approximately 8.20 ppm and the disappearance of the signal at around 3.20 ppm. This change is attributed to the conversion of the primary amine in precursor compound **1** to a secondary amine in ligand **2**, following the incorporation of the triazine core. The ^{13}C NMR spectrum of the 7-chloroquinoline-1,3,5-triazine ligand (**2**) substantiates its successful synthesis by the appearance of the signal at 161.29 ppm assigned to the quaternary carbon of the triazine core (Figure S1).

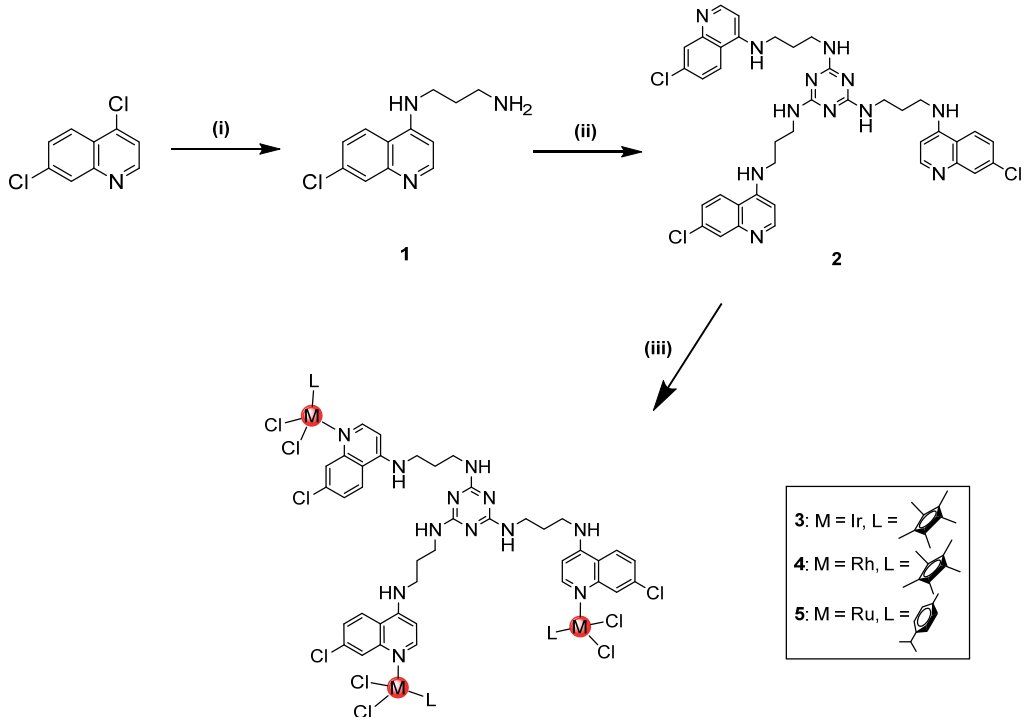

Scheme 1: Synthesis of the 4-aminoquinoline precursor (**1**), the trimeric 4-aminoquinoline-1,3,5-triazine ligand (**2**) and the homo-trinuclear Ir(III), Rh(III) and Ru(II) 4-aminoquinoline-1,3,5-triazine complexes (**3-5**). Reagents and conditions: (i) 1,3-diaminopropane, 120-130 °C, 6-8 h; (ii) cyanuric chloride, NaOH, DMF, MW, 6 bar, 150 °C, 20 min, (iii) $[IrCp^*(\mu\text{-Cl})Cl]_2$, $[RhCp^*(\mu\text{-Cl})Cl]_2$ or $[Ru(p\text{-cymene})(\mu\text{-Cl})Cl]_2$, MeCN or MeOH, r.t., 16 h.

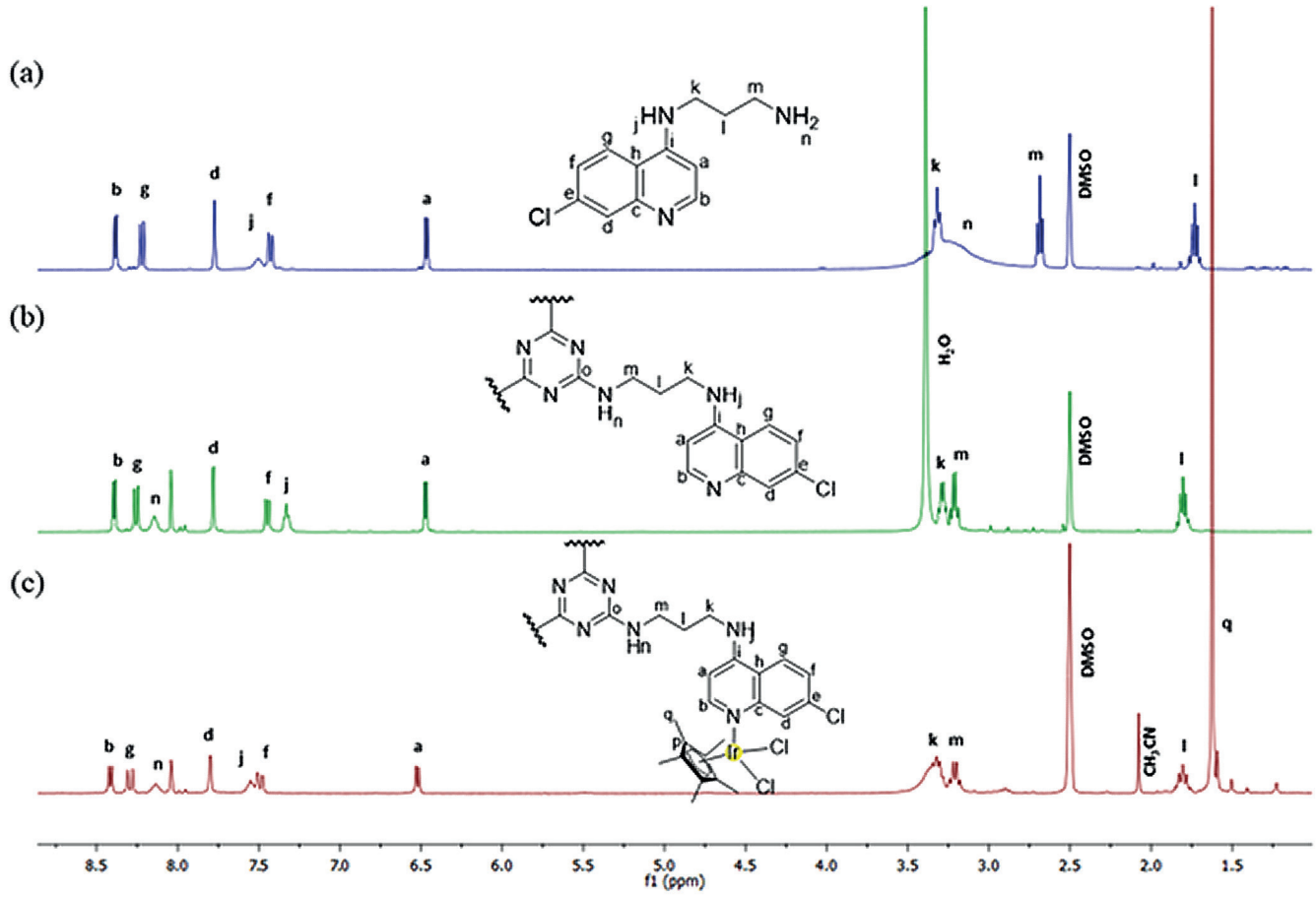

Figure 1: Stacked ^{1}H NMR spectra of (a) aminoquinoline precursor **1**, (b) ligand **2**, and (c) Ir(III) complex, 3•$(CH_3CN)_x$, **3** in DMSO-d_6.

The ^{1}H NMR and infrared spectra, of complexes **3**-**5** are similar, therefore, the spectrum of the Ir(III) complex **3** serves as a representative spectrum for all three trinuclear metal complexes. ^{1}H NMR and IR spectra of trinuclear Rh(III) and Ru(II) metal complexes (**4, 5**) are displayed in the Supplementary Information (Figures S2-S8). The Ir(III) complex, 3•$(CH_3CN)_x$, where x represents the number of acetonitrile molecules per complex unit, was identified based on the ^{1}H NMR spectrum (Figure 1c), which shows the presence of CH_3CN as part of the solvate. For clarity and conciseness, the Ir(III) acetonitrile solvate, 3•$(CH_3CN)_x$, will hereafter be referred to simply as the Ir(III) complex throughout the article. The examination of the ^{1}H NMR spectra of the trinuclear iridium(III) and rhodium(III) 7-chloroquinoline-1,3,5-triazine complexes (**3, 4**) revealed an additional singlet at 1.63 ppm integrating for 45 protons, corresponding to the methyl protons on the Cp* ligands and confirm the complexation of the respective metals to each quinoline motif (Figures 1 and S2).

The ^{1}H NMR spectrum of Ru(II) complex **5** in DMSO-d_6 (Figure S3c) reveals three additional signals compared to the ligand (Figure S3b). These signals, at 5.80 ppm (12 protons), 2.08 ppm (9 protons), and 1.18 ppm (18 protons), correspond to the protons of the p-cymene ligands. While these signals confirm the presence of Ru(II) in the complex, the absence of significant shifts raises questions about the extent of complexation. Further, the lack of expected downfield shifts in the aromatic protons of the quinoline group suggests potential competition from DMSO for coordination with the metal centre, which might lead to ligand dissociation.

The proposed monodentate coordination of the metals to the quinoline-based ligand contributes to the complex's instability, making it easier for the coordinating solvent DMSO to substitute the ligand. This behaviour contrasts with bidentate coordination, which tends to provide greater stability and is less susceptible to solvent exchange, as noted in the literature.[61-66] Previous studies report comparable behaviour in related complexes, including poor solubility and solvent-mediated dissociation.[67-71]

The transition to a non-coordinating solvent, such as MeOH-d_4, provides clearer evidence of metal coordination (Figure S4), confirming that DMSO's coordinating nature impacts the stability of complexes **3**-**5**. This finding underscores the solvent's role in influencing metal-ligand interactions, as documented in previous studies. The Ru(II) complex **5**, unlike the insoluble Ir(III) and Rh(III) analogues, dissolves in non-coordinating solvents like methanol, allowing comprehensive NMR analysis. Notable downfield shifts are observed for all 15 quinoline protons, confirming that metal coordination occurs at the nitrogen atoms of all three quinoline moieties. Additional evidence is provided by the *p*-cymene ligand signals with a multiplet at 2.78 ppm (3 protons, H_q), singlets at 2.20 ppm and 2.19 ppm (6 and 3 protons, respectively, H_u), and a multiplet at 1.26 ppm (18 protons, H_p).

The aromatic signals of the *p*-cymene ring, appearing between 5.23 ppm and 5.71 ppm, show six doublets, each integrating for two protons. This pattern indicates that the three *p*-cymene ligands are in different chemical environments, suggesting the presence of conformers. Changes in H_u signals from one to two singlets and in H_p signals from a doublet to a multiplet upon complex formation further support the existence of conformational isomers. This behaviour is consistent with literature on tri-substituted triazine compounds, where rotational isomerism often results in multiple peaks for a given proton or set of protons.[34,37,72] Additionally, the flexibility of the propyl chain linkers contributes to various conformational and rotational possibilities around the central triazine structure.

In addition to the ^{1}H NMR data, solution-state ^{13}C NMR experiments confirmed the integrity of the Ru(II) complex (**5**). The Ru(II) trinuclear complex, **5**, was the only analogue of the series which was soluble in a non-coordinating solvent (*i.e.* methanol), allowing for facile analysis by solution-state ^{1}H and ^{13}C NMR spectroscopy.

The ^{13}C NMR spectrum (Figure S5) shows an additional ten signals, accounting for the incorporation of the *p*-cymene moieties attached to the Ru(II) metal centres.

Difficulty obtaining conclusive solution-state NMR spectra for the trinuclear complexes (**3, 4**) was due to their poor solubility in all solvents except the extremely polar solvent, dimethylsulfoxide (DMSO). Moreover, the complexes (**3, 4**) exhibited instability in this coordinating solvent, DMSO, which further limited our options. As a result, solid-state ^{1}H NMR and ^{13}C cross polarisation magic angle spinning (CP-MAS) NMR experiments were utilised to substantiate successful synthesis of the Ir(III) and Rh(III) trinuclear complexes (**3, 4**). Solid-state NMR techniques, while offering valuable insights into complex characterisation, present significant challenges due to factors like dipolar coupling and chemical shift anisotropy.[73] These difficulties often result in broad and overlapping signals, making detailed interpretation more complex. Despite these challenges, solid-state ^{1}H NMR can provide general observations about specific spectral regions, while ^{13}C NMR is particularly effective in revealing subtle electronic environment changes, thereby aiding in the understanding of complex formation and metal influence.[74,75] Numerous mono-, di- and tri-substituted triazine compounds' structures have been investigated by solid-state CP-MAS ^{13}C NMR due to the inherent existence of rotational and conformational isomers about the substituted triazine ring.[34-36,72,76,77] Figure S6 and Figure 2 show the ^{1}H NMR and CP-MAS ^{13}C NMR spectra, respectively, of the aminoquinoline-triazine ligand (**2**) and corresponding complexes, **3** and **4**. These spectroscopic results support the successful metal complexation of the aminoquinoline-triazine ligand to each relevant metal centre (Ir(III) or Rh(III)). The ^{1}H and ^{13}C NMR spectra of ligand **2** (Figures S6a and 2a, respectively) yielded broad Gaussian resonances indicative of a disordered and amorphous material thus, offering little detailed structural information. On the other hand, the crystalline metal complexes, **3** and **4**, display sharp resonances typical of ordered materials (Figures 2 and S6). Generally, the more crystalline a substance, the sharper the peaks observed in solid-state NMR spectra. This stark differences in the spectra reflects the disparity in chemical composition between the purely organic ligand and the metallic complexes, as metallic complexes are typically more crystalline due to reduced structural disorder, as discussed in research on the characterisation of various materials, including metal halide perovskites and zeolites.[78-80] The largest peaks observed in th Ir(III) complex and Rh(III) complex ^{1}H NMR spectra (Figures S6b and c) are attributed to the methyl groups on the pentadienyl ring systems, which is consistent with the high number of protons contributing to this signal. Additionally, aromatic protons are identifiable within the range of *ca.* 10 - 6 ppm, with further indications of methylenes in the *ca.* 5 - 3 ppm range and methyls in the *ca.* 2 - 0.8 ppm range.

While the ^{1}H NMR spectra offer limited insight, the ^{13}C NMR spectra (Figure 2) provide more definitive evidence for characterisation. In particular, the pentadienyl signals (C_p and C_q) at 9.48 ppm and 86.1 ppm for the Ir(III) complex (**3**) and at 9.68 ppm and 94.5 ppm for the Rh(III) complex (**4**) support the incorporation of the respective metal centres. Additionally, the shifts in these signals reflect the influence of the different metals used in complex formation, with the signal labelled 'p' showing significantly deshield in the Rh(III) complex compared to the Ir(III).

Notably, the downfield shift of the carbon signal C_b in the complexes (3, 4), compared to the ligand (2) suggest metal coordination to the quinoline nitrogen, with this carbon being most affected electronically due to its proximity to the site of the metal centre. The carbon signal peaks at 162.7 ppm for ligand 2, 161.8 ppm for Ir(III) complex 3 and 161.6 ppm for Rh(III) complex 4 confirm the presence of the triazine structures in all three compounds. The obtained solid-state CP-MAS ^{13}C NMR spectra for the ligand (**2**) and corresponding complexes **3** and **4**, are highly comparable to those published in the literature for tri-substituted triazine based compounds.[34-38,81]

Figure S7 shows the overlapping IR spectra of the starting material, cyanuric chloride, as well as the precursor **1**, the trimeric ligand **2** and the iridium(III) metal complex **3**. The IR spectrum of the ligand (**2**) shows a diagnostic absorption band at 1654 cm^{-1}, corresponding to the imine (C=N) bond of the triazine core, which is not present in the spectrum of precursor **1**, indicating that the desired trimeric compound (**2**) had been formed. Additionally, the spectrum of cyanuric chloride shows a strong ν(C=N) absorption band resonating

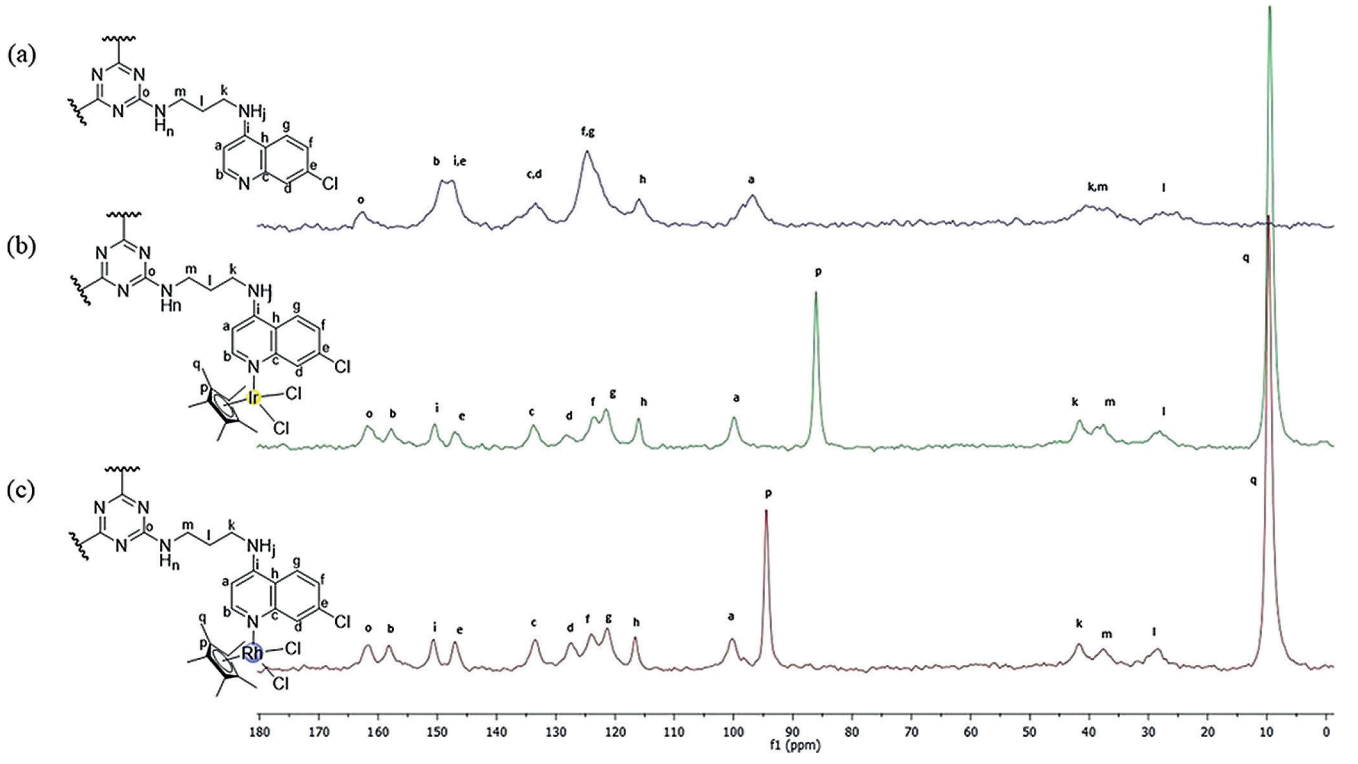

Figure 2: Representative solid-state CP-MAS ^{13}C NMR spectra of (a) 4-aminoquinoline-triazine ligand **2**, (b) Ir(III) trinuclear 4-aminoquinoline-triazine complex **3**, and (c) Rh(III) 4-aminoquinoline-triazine trinuclear complex **4**.

at a comparably lower wavenumber, of 1472 cm^{-1}, than in the spectrum of ligand **2**. This shift of the imine (C=N) absorption band to a higher wavenumber is indicative of the successful hybridisation of the 4-aminoquinoline derivative and the triazine scaffold to form the trimeric ligand **2**.

A comparison of the IR spectra of the trimeric ligand (**2**) and the respective trinuclear Ir(III) aminoquinoline-triazine metal complex (**3**) reveals a shift in the absorption band attributed to the imine (C=N) bond of the quinoline scaffold from *ca.* 1562 cm^{-1} to *ca.* 1589 cm^{-1}, respectively. The shift in vibrational frequencies corroborates the successful coordination of the Ir(III) metal centre to the quinoline nitrogen atom. Metal complexation results in the accumulation of a positive charge on the quinoline nitrogen causing a decrease in the aromaticity of the quinoline core while the bond order of the C=N bond increases which contributes to the shift of the imine band to a higher wavenumber. The IR data seen in Figure S7 and S8 are comparable with those reported in the literature for structurally similar aminoquinoline-1,3,5-triazine complexes.[21,59]

The trimeric aminoquinoline-triazine ligand (**2**) was analysed by LC-MS, as well as high resolution ESI-MS, both operated in the negative-ion mode (Figure S9). The mass spectrum of ligand **2** shows a large degree of fragmentation of the parent ion. The spectral data was likely affected by either the decomposition of compound **2** upon ionisation or the low solubility of the compound (**2**) in the volatile solvents (*i.e.* MeOH or MeCN) utilized for this technique. The mass spectral data yielded a peak at *m/z* 271.2 corresponding to the calculated mass of 271.9 for the ($[M+Cl-2H]^{3-}$) ion fragment. Additionally, a peak is observed at *m/z* 780.8481 corresponding to the calculated mass of 781.2030 which represents the molecular ion ($[M-H]^{-}$). High resolution ESI-MS was also used to validate the structural integrity of the tri-homonuclear half-sandwich Ir(III), Rh(III) and Ru(II) complexes (**3-5**). Similarly, these complexes displayed very poor solubility in the volatile solvents used for this technique. Probable decomposition of the trinuclear complexes (**3-5**) upon ionisation presumably also affected the resulting mass spectral data, causing noticeable fragmentation. The mass spectra of both complexes **3** and **4** (Figures S10 and S11) show peaks corresponding to the molecular ion with the solvent molecule, CH_3CN, and three sodium ions included, $[M + CH_3CN + 3Na^+]^{3+}$. The corresponding *m/z* values for complexes **3** and **4** are 626.1290 and 536.0757, respectively, which correspond to the calculated values of 625.6087 and 536.2987, respectively. The mass spectrum of Ru(II) complex **5** (Figure S12) shows a peak with a *m/z* value of 590.9619, corroborating the calculated mass of 591.1687, which represents the ion fragment of the molecule plus a MeOH solvent molecule and three sodium cations, $[M + MeOH + 3Na^+]^{3+}$.

While this study primarily reports the synthesis and characterisation of trimeric aminoquinoline–triazine ligands and their tri-homonuclear complexes, the complexes however show poor stability in DMSO and insolubility in aqueous media, limiting their biological applicability. Future work focuses on structural modifications to improve solubility in both organic and aqueous solvents, enabling more effective analysis and advancing their potential as chemotherapeutic agents.

CONCLUSION

A new 4-aminoquinoline-1,3,5-triazine ligand (**2**) and a series of three corresponding trinuclear platinum group organometallic complexes (**3-5**) were successfully synthesised. Microwave irradiation was used to ensure complete functionalisation of the triazine core during synthesis of the trimeric ligand, which was followed by a simple entropically driven bridge-splitting reaction to yield the homo-trinuclear complexes. The synthesised compounds were fully characterised using an array of spectroscopic and analytical techniques. All compounds were analysed by infrared spectroscopy to confirm the presence of specific functional groups, while precursor compound **1**, ligand **2** and Ru(II) complex **5** were fully characterised using solution-state NMR (^1H, $^{13}C\{^1H\}$) spectroscopy. Solid-state NMR techniques (CP-MAS ^{13}C and ^1H) were used for the characterisation of complexes **3** and **4**, due to their solubility problems. The solid-state NMR spectra show the crystalline and ordered nature of the Ir(III), and Rh(III) complexes (**3, 4**) compared to the amorphous nature of the organic ligand (**2**), demonstrating a useful characterisation technique for larger multinuclear complexes. The spectroscopic and analytical data obtained attested to the integrity of the proposed structures of the synthesised precursor (**1**), ligand (**2**) and complexes (**3-5**).

This study demonstrated a facile microwave-assisted synthetic procedure for the preparation of a new trimeric ligand and homo-trinuclear organometallic complexes bearing various platinum-group metals. Furthermore, the outlined procedure contributes to the promising yet unexploited research field of multinuclear organometallic complex synthesis.

SUPPLEMENTARY INFORMATION

Supplementary information for this article is provided in the online supplement.

ACKNOWLEDGEMENTS

We gratefully acknowledge and thank the University of Cape Town and the National Research Foundation of South Africa (UID:129288) for financial support.

AUTHORS CONTRIBUTIONS

Paige S. Zinman: Investigation, Data Curation, Writing-Original Draft, Validation, Formal Analysis. **Gregory S. Smith**: Conceptualisation, Resources, Writing-Review and Editing, Supervision, Project Administration, Funding Acquisition.

DECLARATION OF COMPETING OR FINANCIAL INTERESTS

The authors declare that they have no known competing financial interests or personal relationships that could have appeared to influence the work reported in this paper.

DECLARATION OF GENERATIVE AI AND AI-ASSISTED TECHNOLOGIES

AI was not used in the preparation of the manuscript or the interpretation of the data.

AUTHOR ORCID ID

Gregory S. Smith: https://orcid.org/0000-0002-2892-5481

REFERENCES

1. McCusker JK. Electronic structure in the transition metal block and its implications for light harvesting. Science. 2019;363(6426):484–488. https://doi.org/10.1126/science.aav9104.
2. Frei A, Zuegg J, Elliott AG, Baker M, Braese S, Brown C, Chen F, G. Dowson C, Dujardin G, Jung N, et al. Metal complexes as a promising source for new antibiotics. Chem Sci (Camb). 2020 Mar 11;11(10):2627–2639. https://doi.org/10.1039/C9SC06460E.
3. Leung C-H, Zhong H-J, Chan DS-H, Ma D-L. Bioactive iridium and rhodium complexes as therapeutic agents. Coord Chem Rev. 2013;257(11-12):1764–1776. https://doi.org/10.1016/j.ccr.2013.01.034.
4. Esteghamat-Panah R, Hadadzadeh H, Farrokhpour H, Simpson J, Abdolmaleki A, Abyar F. Synthesis, structure, DNA/protein binding, and cytotoxic activity of a rhodium(III) complex with 2,6-bis(2-benzimidazolyl)pyridine. Eur J Med Chem. 2017;127:958–971. https://doi.org/10.1016/j.ejmech.2016.11.005.
5. Monro S, Colón KL, Yin H, Roque J 3rd, Konda P, Gujar S, Thummel RP, Lilge L, Cameron CG, McFarland SA. Transition Metal Complexes and

Photodynamic Therapy from a Tumor-Centered Approach: Challenges, Opportunities, and Highlights from the Development of TLD1433. Chem Rev. 2019;119(2):797–828. https://doi.org/10.1021/acs.chemrev.8b00211.

6. Ndagi U, Mhlongo N, Soliman ME. Metal complexes in cancer therapy – an update from drug design perspective. Drug Des Devel Ther. 2017;11:599–616. https://doi.org/10.2147/DDDT.S119488.
7. Gasser G, Metzler-Nolte N. The potential of organometallic complexes in medicinal chemistry. Curr Opin Chem Biol. 2012;16(1-2):84–91. https://doi.org/10.1016/j.cbpa.2012.01.013.
8. Govender P, Therrien B, Smith GS. Bio-Metallodendrimers – Emerging Strategies in Metal-Based Drug Design. Eur J Inorg Chem. 2012;2012(17):2853–2862. https://doi.org/10.1002/ejic.201200161.
9. Welsh A, Rylands LI, Arion VB, Prince S, Smith GS. Synthesis and antiproliferative activity of benzimidazole-based, trinuclear neutral cyclometallated and cationic, N ^ N-chelated ruthenium(II) complexes. Dalton Trans. 2020;49(4):1143–1156. https://doi.org/10.1039/C9DT03902C.
10. Sun M, Wang C, Sun C-Y, Zhang M, Wang X-L, Su Z-M. Ultra stable multinuclear metal complexes as homogeneous catalysts for visible-light driven syngas production from pure and diluted CO2. J Catal. 2020;385:70–75. https://doi.org/10.1016/j.jcat.2020.03.005.
11. Cerfontaine S, Wehlin SAM, Elias B, Troian-Gautier L. Photostable Polynuclear Ruthenium(II) Photosensitizers Competent for Dehalogenation Photoredox Catalysis at 590 nm. J Am Chem Soc. 2020;142(12):5549–5555. https://doi.org/10.1021/jacs.0c01503.
12. Govender P, Lemmerhirt H, Hutton AT, Therrien B, Bednarski PJ, Smith GS. First- and Second-Generation Heterometallic Dendrimers Containing Ferrocenyl–Ruthenium(II)–Arene Motifs: Synthesis, Structure, Electrochemistry, and Preliminary Cell Proliferation Studies. Organometallics 3. 2014;3:5535. https://dx.doi.org/10.1021/om500809g.
13. Cheng F, He C, Yu S. Two trinuclear Ru(II) complexes of hetero-tritopic bridging ligands: synthesis, characterisation, theoretical calculations, photophysical and electrochemical properties. Transition Met. Chem. 2017;42:395. https://doi.org/10.1007/s11243-017-0142-z.
14. Motimani NM, Ngubane S, Smith GS. Polynuclear heteroleptic ruthenium(II) photoredox catalysts: evaluation in blue-light-mediated, regioselective thiol-ene reactions. Polyhedron. 2022;212:115616. https://doi.org/10.1016/j.poly.2021.115616.
15. Lakshmi Prapurna Y, Raji Reddy C. 1, 2, 3-Triazines and Their Benzo Derivatives. In: Black DS, Cossy J, Stevens CV, editors, Comprehensive Heterocyclic Chemistry IV, Volume 6, Section 2.18. Oxford: Elsevier; 2022. pp. 1007–1051.
16. Fatykhov RF, Chupakhin ON, Rusinov VL, Khalymbadzha IA, Srivastava A, editors. Copper in N-Heterocyclic Chemistry. Oxford: Elsevier; 2021.
17. Singla P, Luxami V, Paul K. Triazine as a promising scaffold for its versatile biological behavior. Eur J Med Chem. 2015;102:39–57. https://doi.org/10.1016/j.ejmech.2015.07.037.
18. Zhou C, Min J, Liu Z, Young A, Deshazer H, Gao T, Chang Y-T, Kallenbach NR. Synthesis and biological evaluation of novel 1,3,5-triazine derivatives as antimicrobial agents. Bioorg Med Chem Lett. 2008;18(4):1308–1311. https://doi.org/10.1016/j.bmcl.2008.01.031.
19. Giampaolo G, Andrea P, Lidia De L. [1,3,5]-Triazine: A Versatile Heterocycle in Current Applications of Organic Chemistry. Curr Org Chem. 2004;8:1497. https://doi.org/10.2174/1385272043369845.
20. Ronchi S, Prosperi D, Compostella F, Panza L. Synthesis of Novel Carborane-hybrids Based on a Triazine Scaffold for Boron Neutron Capture Therapy. Synlett. 2004;2004:1007. https://doi.org/10.1055/s-2004-822897.
21. Melato S, Prosperi D, Coghi P, Basilico N, Monti D. A Combinatorial Approach to 2,4,6-Trisubstituted Triazines with Potent Antimalarial Activity: Combining Conventional Synthesis and Microwave-Assistance. ChemMedChem. 2008;3(6):873–876. https://doi.org/10.1002/cmdc.200700344.
22. Díaz-Ortiz A, Elguero J, de la Hoz A, Jiménez A, Moreno A, Moreno S, Sánchez-Migallón A. Microwave-Assisted Synthesis and Dynamic Behaviour of N2,N4,N6-Tris(1H-pyrazolyl)-1,3,5-triazine-2,4,6-triamines. QSAR Comb Sci. 2005;24(5):649–659. https://doi.org/10.1002/qsar.200420116.
23. Mooibroek TJ, Gamez P. The s-triazine ring, a remarkable unit to generate supramolecular interactions. Inorg Chim Acta. 2007;360(1):381–404. https://doi.org/10.1016/j.ica.2006.07.061.
24. Tahir N, Krishnaraj C, Leus K, Van Der Voort P. Development of Covalent Triazine Frameworks as Heterogeneous Catalytic Supports. Polymers (Basel). 2019;11(8):1326. https://doi.org/10.3390/polym11081326.
25. Kumar D, Khan SI, Ponnan P, Rawat DS. Triazine–pyrimidine based molecular hybrids: synthesis, docking studies and evaluation of antimalarial activity. New J Chem. 2014;38(10):5087–5095. https://doi.org/10.1039/C4NJ00978A.
26. Agarwal A, Srivastava K, Puri SK, Chauhan PM. Syntheses of 2,4,6-trisubstituted triazines as antimalarial agents. Bioorg Med Chem Lett. 2005;15(3):531–533. https://doi.org/10.1016/j.bmcl.2004.11.052.
27. Sreeperumbuduru RS, Abid ZM, Claunch KM, Chen HH, McGillivray SM, Simanek EE. Synthesis and antimicrobial activity of triazine dendrimers with DABCO groups. RSC Adv. 2016;6(11):8806–8810. https://doi.org/10.1039/C5RA10388F.
28. Lim J, Guan B, Nham K, Hao G, Sun X, Simanek EE. Tumor Uptake of Triazine Dendrimers Decorated with Four, Sixteen, and Sixty-Four PSMA-Targeted Ligands: Passive versus Active Tumor Targeting. Biomolecules. 2019;9(9):421. https://doi.org/10.3390/biom9090421.
29. Pennetta C, Bono N, Ponti F, Bellucci MC, Viani F, Candiani G, Volonterio A. Multifunctional Neomycin-Triazine-Based Cationic Lipids for Gene Delivery with Antibacterial Properties. Bioconjug Chem. 2021;32(4):690–701. https://doi.org/10.1021/acs.bioconjchem.0c00616.
30. Klenke B, Stewart M, Barrett MP, Brun R, Gilbert IH. Synthesis and Biological Evaluation of *s* -Triazine Substituted Polyamines as Potential New Anti-Trypanosomal Drugs. J Med Chem. 2001;44(21):3440–3452. https://doi.org/10.1021/jm010854+.
31. El-Faham A, Farooq M, Almarhoon Z, Alhameed RA, Wadaan MAM, de la Torre BG, Albericio F. Di- and tri-substituted s-triazine derivatives: Synthesis, characterisation, anticancer activity in human breast-cancer cell lines, and developmental toxicity in zebrafish embryos. Bioorg Chem. 2020;94:103397. https://doi.org/10.1016/j.bioorg.2019.103397.
32. Al-Khodir FAI, Abumelha HMA, Al-Warhi T, Al-Issa SA. New Platinum(IV) and Palladium(II) Transition Metal Complexes of s-Triazine Derivative: Synthesis, Spectral, and Anticancer Agents Studies. BioMed Res Int. 2019;2019:9835745. https://doi.org/10.1155/2019/9835745.
33. Barakat A, El-Faham A, Haukka M, Al-Majid AM, Soliman SM. *s* -Triazine pincer ligands: synthesis of their metal complexes, coordination behavior, and applications. Appl Organomet Chem. 2021;35(10):e6317. https://doi.org/10.1002/aoc.6317.
34. Birkett HE, Cherryman JC, Chippendale AM, Evans JSO, Harris RK, James M, King IJ, McPherson G. Structural investigations of three triazines: solution-state NMR studies of internal rotation and structural information from solid-state NMR, plus a full structure determination from powder x-ray diffraction in one case. Magn Reson Chem. 2003;41(5):324–336. https://doi.org/10.1002/mrc.1185.
35. Birkett HE, Harris RK, Hodgkinson P, Carr K, Charlton MH, Cherryman JC, Chippendale AM, Glover RP. NMR studies of exchange between triazine rotamers. Magn Reson Chem. 2000;38(7):504–511. https://doi.org/10.1002/1097-458X(200007)38:73.0.CO;2-7.
36. Moreno KX, Simanek EE. Conformational Analysis of Triazine Dendrimers: Using NMR Spectroscopy To Probe the Choreography of a Dendrimer's Dance. Macromolecules. 2008;41(12):4108–4114. https://doi.org/10.1021/ma702143f.
37. Sun R, Wang X, Wang X, Tan B. Three-Dimensional Crystalline Covalent Triazine Frameworks via a Polycondensation Approach. Angew Chem Int Ed. 2022;61(15):e202117668. https://doi.org/10.1002/anie.202117668.
38. Dai J, Li B. Synthesis, thermal degradation, and flame retardance of novel triazine ring-containing macromolecules for intumescent flame retardant polypropylene. J Appl Polym Sci. 2010;116(4):2157–2165. https://doi.org/10.1002/app.31813.
39. Silen JL, Lu AT, Solas DW, Gore MA, MacLean D, Shah NH, Coffin JM, Bhinderwala NS, Wang Y, Tsutsui KT, et al. Screening for Novel Antimicrobials from Encoded Combinatorial Libraries by Using a Two-Dimensional Agar Format. Antimicrob Agents Chemother. 1998;42(6):1447–1453. https://doi.org/10.1128/AAC.42.6.1447.
40. Gewald R, Grunwald C, Egerland U. Discovery of triazines as potent, selective and orally active PDE4 inhibitors. Bioorg Med Chem Lett. 2013;23(15):4308–4314. https://doi.org/10.1016/j.bmcl.2013.05.099.

41. Zacharie B, Abbott SD, Bienvenu J-F, Cameron AD, Cloutier J, Duceppe J-S, Ezzitouni A, Fortin D, Houde K, Lauzon C, et al. 2,4,6-Trisubstituted Triazines as Protein A Mimetics for the Treatment of Autoimmune Diseases. J Med Chem. 2010;53(3):1138–1145. https://doi.org/10.1021/jm901403r.
42. Sunduru N, Gupta L, Chaturvedi V, Dwivedi R, Sinha S, Chauhan PMS. Discovery of new 1,3,5-triazine scaffolds with potent activity against Mycobacterium tuberculosis H37Rv. Eur J Med Chem. 2010;45(8):3335–3345. https://doi.org/10.1016/j.ejmech.2010.04.017.
43. Singh UP, Singh RK, Bhat HR, Subhashchandra YP, Kumar V, Kumawat MK, Gahtori P. Synthesis and antibacterial evaluation of series of novel tri-substituted-s-triazine derivatives. Med Chem Res. 2011;20(9):1603–1610. https://doi.org/10.1007/s00044-010-9446-7.
44. Arya K, Dandia A. Synthesis and cytotoxic activity of trisubstituted-1,3,5-triazines. Bioorg Med Chem Lett. 2007;17(12):3298–3304. https://doi.org/10.1016/j.bmcl.2007.04.007.
45. Chen X, Zhan P, Liu X, Cheng Z, Meng C, Shao S, Pannecouque C, Clercq ED, Liu X. Design, synthesis, anti-HIV evaluation and molecular modeling of piperidine-linked amino-triazine derivatives as potent non-nucleoside reverse transcriptase inhibitors. Bioorg Med Chem. 2012;20(12):3856–3864. https://doi.org/10.1016/j.bmc.2012.04.030.
46. Xiong YZ, Chen FE, Balzarini J, De Clercq E, Pannecouque C. Non-nucleoside HIV-1 reverse transcriptase inhibitors. Part 11: structural modulations of diaryltriazines with potent anti-HIV activity. Eur J Med Chem. 2008;43(6):1230–1236. https://doi.org/10.1016/j.ejmech.2007.08.001.
47. Kaisha ZKK. EP1389617A1. Office EP, editor. Japan; 2006.
48. Li Y, de Kock C, Smith PJ, Guzgay H, Hendricks DT, Naran K, Mizrahi V, Warner DF, Chibale K, Smith GS. Synthesis, Characterisation, and Pharmacological Evaluation of Silicon-Containing Aminoquinoline Organometallic Complexes As Antiplasmodial, Antitumor, and Antimycobacterial Agents. Organometallics. 2013;32(1):141–150. https://doi.org/10.1021/om300945c.
49. Lauria A, La Monica G, Bono A, Martorana A. Quinoline anticancer agents active on DNA and DNA-interacting proteins: from classical to emerging therapeutic targets. Eur J Med Chem. 2021;220:113555. https://doi.org/10.1016/j.ejmech.2021.113555.
50. Verbaanderd C, Maes H, Schaaf MB, Sukhatme VP, Pantziarka P, Sukhatme V, Agostinis P, Bouche G. Repurposing Drugs in Oncology (ReDO) — chloroquine and hydroxychloroquine as anti-cancer agents. Ecancermedicalscience. 2017;11:781. https://doi.org/10.3332/ecancer.2017.781.
51. Manohar S, Pepe A, Vélez Gerena CE, Zayas B, Malhotra SV, Rawat DS. Anticancer activity of 4-aminoquinoline-triazine based molecular hybrids. RSC Adv. 2014;4(14):7062. https://doi.org/10.1039/c3ra45333b.
52. Manohar S, Khan SI, Rawat DS. Synthesis of 4-aminoquinoline-1,2,3-triazole and 4-aminoquinoline-1,2,3-triazole-1,3,5-triazine Hybrids as Potential Antimalarial Agents. Chem Biol Drug Des. 2011;78(1):124–136. https://doi.org/10.1111/j.1747-0285.2011.01115.x.
53. Melato S, Coghi P, Basilico N, Prosperi D, Monti D. Novel 4-Aminoquinolines through Microwave-Assisted S_NAr Reactions: a Practical Route to Antimalarial Agents. Eur J Org Chem. 2007;2007(36):6118–6123. https://doi.org/10.1002/ejoc.200700612.
54. Srivastava V, Lee H. Chloroquine-based hybrid molecules as promising novel chemotherapeutic agents. Eur J Pharmacol. 2015;762:472–486. https://doi.org/10.1016/j.ejphar.2015.04.048.
55. Bennett MA, Smith AK. Arene ruthenium(II) complexes formed by dehydrogenation of cyclohexadienes with ruthenium(III) trichloride. J Chem Soc, Dalton Trans. 1974;2(2):233. https://doi.org/10.1039/dt9740000233.
56. Kang JW, Moseley K, Maitlis PM. Pentamethylcyclopentadienylrhodium and -iridium halides. I. Synthesis and properties. J Am Chem Soc. 1969;91(22):5970–5977. https://doi.org/10.1021/ja01050a008.
57. Musonda CC, Gut J, Rosenthal PJ, Yardley V, Carvalho de Souza RC, Chibale K. Application of multicomponent reactions to antimalarial drug discovery. Part 2: new antiplasmodial and antitrypanosomal 4-aminoquinoline γ- and δ-lactams via a 'catch and release' protocol. Bioorg Med Chem. 2006;14(16):5605–5615. https://doi.org/10.1016/j.bmc.2006.04.035.
58. Natarajan JK, Alumasa JN, Yearick K, Ekoue-Kovi KA, Casabianca LB, de Dios AC, Wolf C, Roepe PD. 4- *N* -, 4- *S* -, and 4- *O* -Chloroquine Analogues: Influence of Side Chain Length and Quinolyl Nitrogen p K_a on Activity vs Chloroquine Resistant Malaria. J Med Chem. 2008;51(12):3466–3479. https://doi.org/10.1021/jm701478a.
59. Melis DR, Barnett CB, Wiesner L, Nordlander E, Smith GS. Quinoline-triazole half-sandwich iridium(III) complexes: synthesis, antiplasmodial activity and preliminary transfer hydrogenation studies. Dalton Trans. 2020;49(33):11543–11555. https://doi.org/10.1039/D0DT01935F.
60. Baartzes N, Jordaan A, Warner DF, Combrinck J, Taylor D, Chibale K, Smith GS. Antimicrobial evaluation of neutral and cationic iridium(III) and rhodium(III) aminoquinoline-benzimidazole hybrid complexes. Eur J Med Chem. 2020;206:112694. https://doi.org/10.1016/j.ejmech.2020.112694.
61. Munakata M, Kitagawa S. Coordination power series of solvents. Inorg Chim Acta. 1990;169(2):225–234. https://doi.org/10.1016/S0020-1693(00)80522-8.
62. Burger K. Solvation Ionic and Complex Formation Reactions in Non-Aqueous Solvents : Experimental Methods for Their Investigation. 1st ed. Budapest: Elsevier Science; 2012. p. 42.
63. Ahrland S, Björk N-O. Influence of the solvent on the stability of metal ion complexes. Coord Chem Rev. 1975;16(1-2):115–127. https://doi.org/10.1016/S0010-8545(00)80288-X.
64. Kleinmaier R, Arenz S, Karim A, Carlsson A-CC, Erdélyi M. Solvent effects on ^{15} N NMR coordination shifts. Magn Reson Chem. 2013;51(1):46–53. https://doi.org/10.1002/mrc.3907.
65. Singh R, Kociok-Köhn G, Singh K, Pandey SK, Singh L. Influence of ligand coordination, solvent, and non-covalent interaction on the structural outcomes in coordination polymers with direct Cd(II)-alkanesulfonate bonds: A combined experimental and computational study. J Solid State Chem. 2019;280:120992. https://doi.org/10.1016/j.jssc.2019.120992.
66. Baartzes N. Development of aminoquinoline-benzimidazole hybrids and their organometallic complexes as antimicrobial agents against Plasmodium falciparum and Mycobacterium tuberculosis. PhD thesis, University of Cape Town; 2019.
67. Patra M, Joshi T, Pierroz V, Ingram K, Kaiser M, Ferrari S, Spingler B, Keiser J, Gasser G. DMSO-Mediated Ligand Dissociation: Renaissance for Biological Activity of *N* -Heterocyclic-[Ru(η ^{6} -arene)Cl $_2$] Drug Candidates. Chemistry. 2013;19(44):14768–14772. https://doi.org/10.1002/chem.201303341.
68. Díaz-Torres R, Alvarez S. Coordinating ability of anions and solvents towards transition metals and lanthanides. Dalton Trans. 2011;40(40):10742. https://doi.org/10.1039/c1dt11000d.
69. Rancan M, Carlotto A, Bottaro G, Armelao L. Effect of Coordinating Solvents on the Structure of Cu(II)-4,4'-bipyridine Coordination Polymers. Inorganics (Basel). 2019;7(8):103. https://doi.org/10.3390/inorganics7080103.
70. Sian L, Dall'Anese A, Macchioni A, Tensi L, Busico V, Cipullo R, Goryunov GP, Uborsky D, Voskoboynikov AZ, Ehm C, et al. Role of Solvent Coordination on the Structure and Dynamics of *ansa* -Zirconocenium Ion Pairs in Aromatic Hydrocarbons. Organometallics. 2022;41(5):547–560. https://doi.org/10.1021/acs.organomet.1c00653.
71. Payehghadr M, Hashemi S. Solvent effect on complexation reactions. J Incl Phenom Macrocycl Chem. 2017;89(3-4):253–271. https://doi.org/10.1007/s10847-017-0759-8.
72. Loeser E, Babiak S. Correlations between conformational isomerism and chromatographic diastereoselectivity of bis amino amide s-triazine derivatives. J Chromatogr A. 2011;1218(48):8672–8678. https://doi.org/10.1016/j.chroma.2011.10.023.
73. Polenova T, Gupta R, Goldbourt A. Magic Angle Spinning NMR Spectroscopy: A Versatile Technique for Structural and Dynamic Analysis of Solid-Phase Systems. Anal Chem. 2015;87(11):5458–5469. https://doi.org/10.1021/ac504288u.
74. Hanrahan MP, Venkatesh A, Carnahan SL, Calahan JL, Lubach JW, Munson EJ, Rossini AJ. Enhancing the resolution of ^{1} H and ^{13} C solid-state NMR spectra by reduction of anisotropic bulk magnetic susceptibility broadening. Phys Chem Chem Phys. 2017;19(41):28153–28162. https://doi.org/10.1039/C7CP04223J.

75. Kolbe F, Ehren HL, Kohrs S, Butscher D, Reiß L, Baldus M, Brunner E. Solid-state NMR spectroscopic studies of 13C,15N,29Si-enriched biosilica from the marine diatom Cyclotella cryptica. Discov Mater. 2021;1(1):3. https://doi.org/10.1007/s43939-020-00003-7.
76. Kushwaha N, Sharma C. The Chemistry of Triazine Isomers: Structures, Reactions, Synthesis and Applications. Mini Rev Med Chem. 2021;20(20):2104–2122. https://doi.org/10.2174/1389557520666200729160720.
77. Uccello-Barretta G, Iuliano A, Franchi E, Balzano F, Salvadori P. Di- and Tri-1-(1-naphthyl)ethylamino-Substituted 1,3,5-Triazine Derivatives: A New Class of Versatile Chiral Auxiliaries for NMR Spectroscopy. J Org Chem. 1998;63(25):9197–9203. https://doi.org/10.1021/jo9806153.
78. Wang W, Xu J, Deng F. Recent advances in solid-state NMR of zeolite catalysts. Natl Sci Rev. 2022;9(9):nwac155. https://doi.org/10.1093/nsr/nwac155.
79. Dahlman CJ, Kubicki DJ, Reddy GNM. Interfaces in metal halide perovskites probed by solid-state NMR spectroscopy. J Mater Chem A Mater Energy Sustain. 2021;9(35):19206–19244. https://doi.org/10.1039/D1TA03572J.
80. Yusuf VF, Malek NI, Kailasa SK. Review on Metal–Organic Framework Classification, Synthetic Approaches, and Influencing Factors: Applications in Energy, Drug Delivery, and Wastewater Treatment. ACS Omega. 2022;7(49):44507–44531. https://doi.org/10.1021/acsomega.2c05310.
81. Song Y, Yang X, Chen X, Nie H, Byrn S, Lubach JW. Investigation of Drug–Excipient Interactions in Lapatinib Amorphous Solid Dispersions Using Solid-State NMR Spectroscopy. Mol Pharm. 2015;12(3):857–866. https://doi.org/10.1021/mp500692a.